Modern techniques for effective wind load distributions on large roofs

John D. Holmes[1)]

JDH Consulting, Mentone, Victoria 3194, Australia
[1)] *john.holmes@jdhconsult.com*

ABSTRACT

Large roofs on sports stadiums, and other large public venues, have proliferated in the last twenty years. The determination of wind loads for the design of the supporting structures cannot generally be handled by wind loading codes and standards. This paper describes some techniques that have been developed for determination of wind loads in the structural members of such roofs, and for determination of effective static wind load distributions. These techniques consider separately the three components of wind loading: the mean or steady state wind pressure, the fluctuating quasi-steady or background component, and the resonant contributions produced by structural vibrations. Some applications of the methods are discussed.

1. INTRODUCTION

In the last twenty years there has been a huge increase in the number of covered sports venues constructed around the world. For example, during this period in the city of Melbourne, Australia, a multi-sport 50,000 seat stadium with a fully closable roof, a football (soccer) and rugby arena (30,000 seat), and two tennis arenas with movable roofs, and an aquatic centre, have all been newly constructed. The historic Melbourne Cricket Ground (100,000 seat approximately) has also been re-built with fully-covered accommodation during this period. Similar developments have occurred in other parts of the world.

Wind loading for the large roofs on these facilities has generally been a challenge for design engineers. Structural engineers usually do not have the background or expertise to go much beyond the provisions of wind loading codes and standards, and turn to wind engineers for input on wind loads. This has usually involved the use of boundary-layer wind tunnels, now commonly used around the world.

Contrary to the perceptions of some, large roofs on sports arenas, and similar-sized roofs such as convention centres, are not generally dynamically wind-sensitive. There are exceptions such as very large roofs with low natural frequencies and roofs with unusually flexible support systems, including some roofs cantilevered from one side.

[1)] Director

However, a special challenge in determination of wind loads results from the influence lines for many load effects (e.g. internal shear forces, axial forces and bending moments) having both positive and negative values. This will lead to upward-acting net wind pressure on one part of a roof having an opposite effect on an internal force to that of an upward-acting net pressure on a different part of the roof. As a result the simple quasi-steady approach to wind loading adopted by most codes and standards, although adequate for small structures, can produce large errors in wind load effects in large roofs. For the same reason 'gust loading factor' methods as widely used for tall buildings and towers, are also not applicable to large roofs.

Traditional aeroelastic structural wind-tunnel models of large roofs, as commonly used in the 1970s and 1980s, had major disadvantages in that they were strongly dependent on the structural system, and thus require the structural design to be complete before a wind-tunnel model can be constructed. They were primarily used to measure deflections (a serviceability design criterion), and they were not able to give realistic loading distributions for the design of the structure.

This paper will describe the bases for modern wind-tunnel techniques, developed in the last twenty years, for determination of wind loads and effective static wind load distributions, on large roofs, and discuss some anecdotal case studies, from the author's experience.

2. COMPONENTS OF WIND LOADING

Wind load effects, and the wind load distributions producing them, can conveniently be divided into three components:

- The mean or static component
- The background fluctuating component
- Resonant components

The first two can be grouped together as 'quasi-static' components.

Two methods are possible to determine the effective static distributions for the quasi-static components:

- A direct approach in which simultaneous time histories of fluctuating pressures from the whole roof are recorded and stored. These are subsequently weighted with structural influence coefficients to obtain time histories of load effects. The instantaneous pressure distributions, coinciding with peak load effects, are then identified and averaged.

- In the other approach, correlations between pressure fluctuations at different parts of the roof are obtained, and expected pressure distributions corresponding to peak load effects are obtained by calculation.

The first method is commonly used in North America and the U.K. for derivation of wind loads for actual large roof structures, whereas the second method has generally been adopted in Australia and Germany. The latter approach is discussed in detail in a later section of this paper.

Although the mean and background load distributions result directly from wind pressures, the effective loading distribution for the resonant loading is an *inertial* loading, proportional to mass, acceleration, and the mode shape coordinate for the particular mode of vibration being considered. This is quite similar to that used in design for seismic loads.

The resonant components are sensitive to the assumed level of damping (both structural and aerodynamic). The structural damping is not well known for actual large roofs, so that a high degree of accuracy in incorporating the resonant components is usually not warranted. The incorporation of the resonant contributions into the analysis is discussed in a subsequent section.

3. MEAN AND BACKGROUND COMPONENTS

The second technique described in the previous section, involves the measurement of correlation coefficients for panel pressures from rigid wind-tunnel models and the determination of structural influence coefficients by the designers, and the use of Kasperski's Load Response Correlation (LRC) equation (Kasperski, 1992; Kasperski and Niemann, 1992) to determine effective static load distributions. However there are some variations in the subsequent analysis techniques. In some cases, Proper Orthogonal Decomposition (POD) (Holmes 1990, 1992) can be used to simplify the calculations.

The LRC method gives an expected effective static load distribution corresponding to a particular load effect or response, r, with an influence coefficient $\beta_r(x)$, i.e. the value of r when a unit load is applied at position, x. In practice, the rigid pressure model is divided into a number of panels, N, with the number of panels dependent on the structural system. Influence coefficients for particular responses of interest (e.g. axial or shear forces, bending moments or deflections) are derived by the structural engineer, by applying a series of patch loads, each one corresponding to a uniformly distributed load applied to the wind tunnel model panel. The influence coefficient vector for each response will have N values.

For a structure of length, L, the instantaneous value of r is:

$$r(t) = \int_0^L p(x,t)\beta_r(x)dx \qquad (1)$$

where $p(x,t)$ is the fluctuating pressure at position x, where $0 < x < L$.

The mean value of *r* is: $\bar{r} = \int_0^L \bar{p}\,(x).\,\beta_r(x)\,dx$ (2)

By covariance integration (Holmes and Best, 1981), the standard deviation of *r* is given by:

$$\sigma_r = \left[\int_0^L \int_0^L \overline{p(x)p(x')}\;\beta_r(x)\beta_r(x')\,dx\,dx'\right]^{1/2} \quad (3)$$

The expected maximum value of *r* is given by:

$$\hat{r} = \bar{r} + g_B\,\sigma_r \quad (4)$$

where g_B is a peak factor, 'B' denoting background response.

The LRC formula for the distribution of $p(x)$ corresponding to $\hat{r}$ is:

$$[p(x)]_{\hat{r}} = \bar{p}(x) + g_B\rho_{pr}(x)\sigma_p(x) \quad (5)$$

where $\rho_{pr}(x)$ is the correlation coefficient between $p(x,t)$ and $r(t)$, given by:

$$\rho_{pr}(x) = \frac{\overline{p(x,t)\int_0^L p(x',t).\beta_r(x')dx'}}{\sigma_p\;\sigma_r} = \frac{\int_0^L \overline{p(x,t).p(x',t)}\beta_r(x')\,dx'}{\sigma_p\;\sigma_r} \quad (6)$$

where σ_r is given by Equation (3).

Note that the numerator in Equation (6) remains a function of position, x.

That Equation (5) is correct can be demonstrated, by computing the peak value, $\hat{r}$, from it.

Thus, $\hat{r} = \int_0^L [p(x)]_{\hat{r}}\,\beta_r(x)dx = \int_0^L \left[\bar{p}(x) + g_B\,\rho_{pr}(x)\sigma_p(x)\right]\beta_r(x)dx$

$$= \int_0^L \bar{p}\,(x)\,\beta_r(x)dx + g_B\frac{\int_0^L\left\{\int_0^L \overline{p(x,t).p(x',t)}\;\beta_r(x')dx'\right\}\beta_r(x)dx}{\sigma_r}$$

$$= \bar{r} + g_B\frac{{\sigma_r}^2}{\sigma_r} \quad \text{(using Equation (3))}$$

$$= \bar{r} + g_B\sigma_r \quad \text{(i.e. Equation (4))}$$

For a roof divided into N discrete panels, Equations (6) and (3) can be re-written as a finite summations:

$$\rho_{p_i,r} = \frac{\sum_{j=1}^{N} \overline{p_i(t).p_j(t)}\,\beta_j}{\sigma_{p_i}\sigma_r} \tag{7}$$

$$\sigma_r = \sum_{i=1}^{N}\sum_{j=1}^{N} \overline{p_i(t).p_j(t)}\beta_i\,\beta_j \tag{8}$$

i and j represent panel numbers, N is the total number of panels.
β_i is the influence coefficient for panel, i, on the load effect, r, and incorporates the area of the panel - that is, β_i is the value of r when a uniformly distributed 'patch load' of unit magnitude is applied to the panel.

The summations in Equations (7) and (8) can be simplified by use of the eigenvalues and eigenvectors of the covariance matrix ($\overline{p_i(t).p_j(t)}$, for $i = 1, N$ and $j = 1, N$) (see Holmes and Best (1981), and Holmes (1990, 2002). However, this will not be discussed further in this paper.

4. RESONANT COMPONENT

The effective load distribution due to the resonant part of the loading is given, to a good approximation, by the distribution of inertial forces over a roof. This is based on the assumption that the fluctuating wind forces at the resonant frequency are balanced by the damping forces, once a stable amplitude of vibration has been established.

Thus, an equivalent load distribution for the resonant response in mode 1, $p_R(x)$, is given by:

$$p_R(x) = g_R\, m(x)(2\pi n_1)^2 \sqrt{\overline{a_1{}'^2}}\;\mu_1(x) \tag{9}$$

where g_R is the peak factor for resonant response; $m(x)$ is a mass per unit length; n_1 is the first mode natural frequency; $\sqrt{\overline{a_1{}'^2}}$ is the r.m.s. modal coordinate (resonant contribution only), and $\mu_1(x)$ is the mode shape for the first mode of vibration.

Determination of the r.m.s. modal coordinate requires knowledge of the spectral density of the exciting forces, the correlation of those forces at the natural frequency (or aerodynamic admittance), and the modal damping and stiffness.

For low damping ratios, the mean square resonant modal coordinate for the 1st mode of vibration is to a good approximation:

$$\overline{a_1'^2} = \frac{[\pi n_1 S_{F1}(n_1)]}{4 K_1^2 \zeta_1} \tag{10}$$

where,

a_1 is the generalized coordinate for the 1st mode of vibration;
n_1 is the natural frequency of the 1st mode,
K_1 is the generalized stiffness equal to ($\omega_1^2 G_1$),
ω_1 (= $2\pi n_1$) is the circular frequency,
G_1 is the generalized mass,
ζ_1 is the critical damping ratio for the 1st mode,
$S_{F1}(n)$ is the power spectral density of the generalized force for the first mode.

The mean square fluctuating value of a load effect, r, resulting from the resonant response in mode 1, can be written:

$$\sigma_{r,R1}^2 = \alpha_1^2 \omega_1^4 \overline{a_1'^2} \tag{11}$$

ω_1 is the circular frequency in mode 1 (= $2\pi n_1$)
α_1 is the integral: $\int_0^L m(x)\, \mu_1(x) \beta_r(x) dx$
$m(x)$ is the mass per unit length for a continuous structure
$\mu_1(x)$ is the mode shape for the first mode of vibration
$\beta_r(x)$ is the influence line for the load effect in question.

Equation (11) indicates that the resonant contribution to a load effect depends strongly on the value of α_1 – i.e. the coincidence of the influence line and the mode shape.

In the case of a roof divided into N discrete panels, α_1 can be written:

$$\alpha_1 = \sum_{i=1}^{N} m_i \mu_{1,i} \beta_i \tag{12}$$

where $\mu_{1,i}$ is the mode shape deflection averaged over the area of panel, i

The total peak response can be estimated by:

$$\hat{r}_T = \bar{r} + \sqrt{\hat{r}_B^2 + \hat{r}_R^2} = \bar{r} + \sqrt{g_B^2 \sigma_B^2 + g_R^2 \sigma_{R,1}^2} \tag{13}$$

The peak factor for the resonant response, g_R, is given by (Davenport, 1964):

$$g_R = \sqrt{(2\ log_e n_1 T} + \frac{0.5772}{\sqrt{(2\ log_e n_1 T}} \quad (14)$$

5. COMBINED EFFECTIVE STATIC LOAD DISTRIBUTIONS

The correct method of combining effective static load distributions for mean, background and resonant components (one mode) is as follows (Holmes, 2002):

$$p_c(x) = \bar{p}(x) + W_B p_B(x) + W_R p_R(x) \quad (15)$$

The absolute values of the weighting factors W_B and W_R are given by:

$$|W_{BR}| = \frac{g_B \sigma_{r,B}}{\left(g_B{}^2 \sigma_{r,B}{}^2 + g_R{}^2 \sigma_{r,R}{}^2\right)^{1/2}}$$

$$|W_R| = \frac{g_R \sigma_{r,R}}{\left(g_B{}^2 \sigma_{r,B}{}^2 + g_R{}^2 \sigma_{r,R}{}^2\right)^{1/2}} \quad (16)$$

Equation (15) can be validated by multiplying both sides by the influence line and integrating over the structure. The sign of W_B depends on the sign of g_B, i.e. on whether a maximum or minimum response is being considered. The sign of W_R depends on the sign of α_1, and will differ from the sign of W_B, if α_1 is negative.

To incorporate additional resonant modes, additional terms can be added to Eq. (15).

i.e. $$p_c(x) = \bar{p}(x) + W_B p_B(x) + W_{R1} p_{R1}(x) + W_{R2} p_{R2}(x) + etc. \quad (17)$$

where,

$$|W_{R1}| = \frac{g_{R1} \sigma_{r,R1}}{\left(g_B{}^2 \sigma_{r,B}{}^2 + g_{R1}{}^2 \sigma_{r,R1}{}^2 + g_{R2}{}^2 \sigma_{r,R2}{}^2\right)^{1/2}}$$

$$|W_{R2}| = \frac{g_{R2} \sigma_{r,R2}}{\left(g_B{}^2 \sigma_{r,B}{}^2 + g_{R1}{}^2 \sigma_{r,R1}{}^2 + g_{R2}{}^2 \sigma_{r,R2}{}^2\right)^{1/2}} \quad (18)$$

6. APPLICATIONS AND CASE STUDIES

In this section, the results of wind loading studies on examples of actual stadium roofs are used to illustrate the principles and techniques discussed in previous sections of this paper.

6.1 Pressure measurement

The methods described in the previous sections require pressure measurements on rigid wind-tunnel models of a stadium roof. Unless parts of the roof are structurally

independent, this normally requires the whole roof to be equipped with pressure taps, so that simultaneous fluctuating pressures can be measured. To reduce the number of pressure measurement channels, pneumatic averaging by means of manifolds can be used so that the pressure measurement is carried out on a finite number of panels.

Figure 1 shows the pressure measurement panels used for a very large roof with a single integrated structural support system. In that case over one hundred panels were used for the upper surface pressure measurements. Pressures for each panel were obtained by pneumatically averaging fluctuating pressures from four taps within each panel using an approach originally suggested by Surry and Stathopoulos (1977). Some examples of pneumatic averagers are shown in Figure 2. The frequency response of the tubing systems used for these measurements needs careful design to avoid introducing unwanted 'organ pipe' resonances and to ensure that the amplitude and phase responses are adequate up to a sufficient frequency. Holmes and Lewis (1987) describe methods by which such systems can be designed.

Figure 3 shows another roof which has four separate fixed roofs on four sides of the stadium together with a moving roof. Tubing can be seen connecting the manifolded area-averaged pressures to pressure sensors (not shown). In that example only half the fixed roof, plus the moving part was equipped with pressure taps. In order to minimise the amount of pressure tubing under the moving roof in the open position (and thus allow free flow of air between the moving roof and the fixed roof underneath), the pressure panels of the moving roof were internally manifolded through machined channels in the thickness of the model roof, in order to separate the pressure measurements on the top and bottom surfaces.

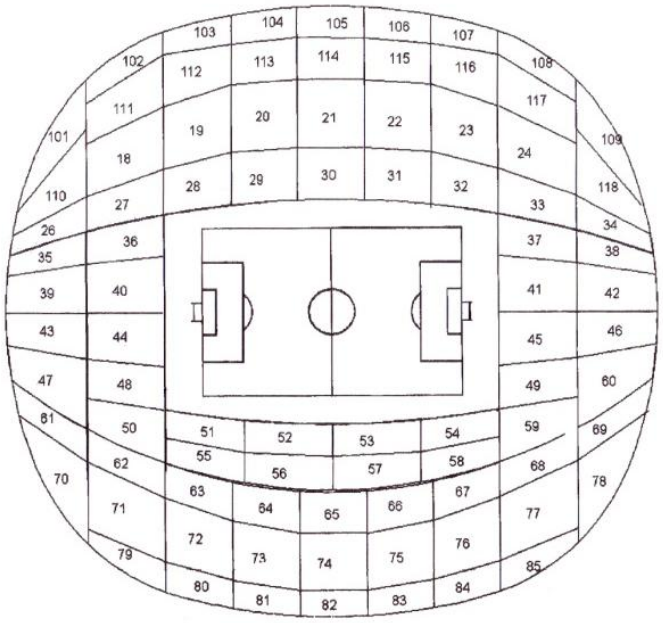

Fig. 1 Panel layout for pressure measurements on a model of large stadium roof

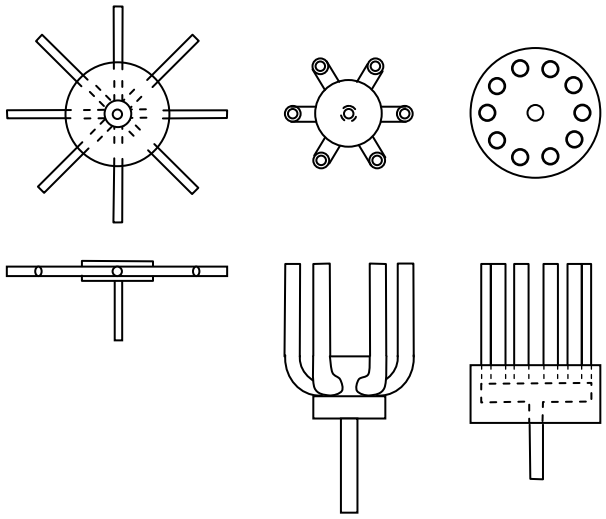

Fig. 2 Some examples of pneumatic averagers for combining pressures from several pressure taps on wind-tunnel models

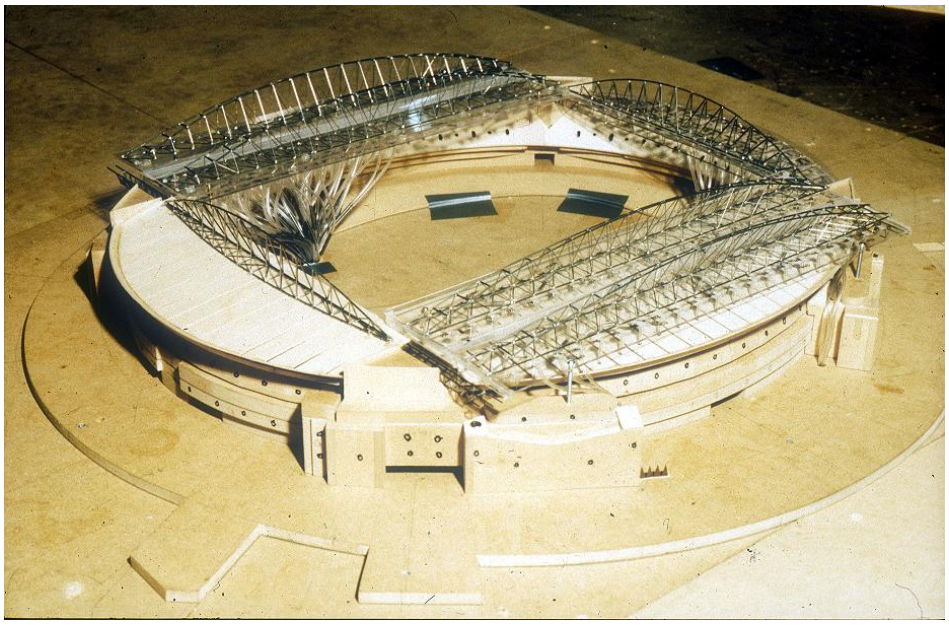

Fig. 3 Example of a wind-tunnel model of a stadium with fixed and moving roofs

6.2 Pressure correlations

An essential component of the LRC method described in Section 3 is a matrix of co-variances, or correlation coefficients, for fluctuating pressures on every pair of pressure panels of an instrumented roof model (see the numerator of Eqn (7)).

An example of a matrix of correlation coefficients is shown in Table I. The diagonal values are unity, and usually the values decrease in magnitudes as the spacing between panels increases. This example includes internal pressures which were measured as a single panel.

Table I. Example of a matrix of correlations between panel pressures on a large roof

Panel	**1**	**2**	**3**	**4**	**5**	**6**	**7**	**8**	**9**	**10**	**11**	**12**	**13**	**14**	**15**	**int**
1	**1.00**	0.74	0.47	0.83	0.68	0.33	0.64	0.49	0.44	0.22	0.41	0.30	0.40	0.43	0.33	0.12
2	0.74	**1.00**	0.68	0.69	0.76	0.53	0.59	0.53	0.53	0.45	0.56	0.51	0.54	0.56	0.46	0.33
3	0.47	0.68	**1.00**	0.41	0.55	0.65	0.41	0.33	0.44	0.73	0.56	0.65	0.51	0.51	0.45	0.55
4	0.83	0.69	0.41	**1.00**	0.71	0.30	0.76	0.54	0.45	0.15	0.36	0.27	0.38	0.45	0.32	0.06
5	0.68	0.76	0.55	0.71	**1.00**	0.53	0.69	0.67	0.64	0.32	0.54	0.49	0.58	0.63	0.52	0.25
6	0.33	0.53	0.65	0.30	0.53	**1.00**	0.40	0.35	0.49	0.64	0.43	0.79	0.44	0.55	0.42	0.54
7	0.64	0.59	0.41	0.76	0.69	0.40	**1.00**	0.75	0.64	0.21	0.37	0.37	0.40	0.56	0.38	0.11
8	0.49	0.53	0.33	0.54	0.67	0.35	0.75	**1.00**	0.81	0.19	0.41	0.38	0.48	0.69	0.47	0.11
9	0.44	0.53	0.44	0.45	0.64	0.49	0.64	0.81	**1.00**	0.33	0.47	0.51	0.53	0.78	0.54	0.24
10	0.22	0.45	0.73	0.15	0.32	0.64	0.21	0.19	0.33	**1.00**	0.53	0.70	0.46	0.46	0.40	0.64
11	0.41	0.56	0.56	0.36	0.54	0.43	0.37	0.41	0.47	0.53	**1.00**	0.53	0.74	0.52	0.56	0.35
12	0.30	0.51	0.65	0.27	0.49	0.79	0.37	0.38	0.51	0.70	0.53	**1.00**	0.57	0.62	0.53	0.56
13	0.40	0.54	0.51	0.38	0.58	0.44	0.40	0.48	0.53	0.46	0.74	0.57	**1.00**	0.59	0.73	0.32
14	0.43	0.56	0.51	0.45	0.63	0.55	0.56	0.69	0.78	0.46	0.52	0.62	0.59	**1.00**	0.66	0.30
15	0.33	0.46	0.45	0.32	0.52	0.42	0.38	0.47	0.54	0.40	0.56	0.53	0.73	0.66	**1.00**	0.31
int	0.12	0.33	0.55	0.06	0.25	0.54	0.11	0.11	0.24	0.64	0.35	0.56	0.32	0.30	0.31	**1.00**

Another important input for the LRC approach comprises the influence coefficients for a number of key load effects for the structural support system(i.e β_i and β_j in Eq. (8)) . These are normally obtained by the structural designer by applying a uniformly distributed 'patch' load to the area corresponding to each panel of the wind-tunnel model and obtaining, by a structural analysis, the key load effects, such as axial forces in tension and compression members, bending moments in flexural members, or support reactions. Deflections can also be included if the serviceability performance of the structure is required to be investigated.

Examples of influence coefficients for a deflection and the axial force in the top chord of a truss are shown in Table II. These values represent the deflection and a truss force, as a uniformly distributed panel load of unit magnitude is applied in turn to every pressure panel on the roof.

Table II. Example of influence coefficients for two load effects on a large roof

Loaded Panel	Influence Coefficient for deflection at Panel 8 (mm)	Influence Coefficient for force in top chord of truss (kN)
1	6.1	580
2	2.1	331
3	-0.1	70
4	111.9	2705
5	68.1	1760
6	28.1	770
7	1.6	37
8	281.3	1872
9	140.4	1210
10	39.5	533
11	0.9	28
12	91.6	367
13	49.9	184
14	11.1	418
15	-614.7	-4612
16	-217.7	-6253

6.4 Examples of an effective static load distributions

An example of an effective static load distribution for the mean and background components of pressure associated with the peak value of a force in a particular structural member is shown in Figure 4. Note that there are different distributions corresponding to the maximum and minimum values of any load effect. Clearly a large number of effective load distributions can be generated depending on how many critical load effects are selected for study. However many of these are similar to each other and 'enveloping' of the distributions for a group of load effects can be carried out in order to generate a manageable number for the structural designer to design the whole structure.

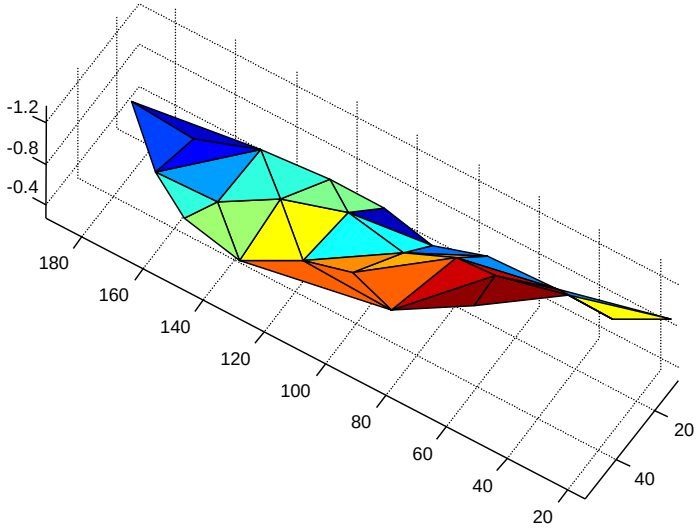

Fig. 4 Critical upwards pressure distribution for a member in a roof structure

Figure 5 compares an effective static load distributions calculated by the LRC formula (Equation (5)) shown as the dashed pink lines, and by the direct method, shown by the green line. They are not exactly the same as the LRC-correlation approach incorporates more averaging, and statistical peak factors (i.e. g_B in Eqn. (5)); however the agreement is good. Since it is based on correlations, the former method gives a more statistically stable result, than the direct or 'conditional sampling' approach, which suffers from significant sampling errors, unless some averaging process is used. Also shown in Figure 5 are the extreme pressure limits of pressure, i.e. the maximum and minimum non-simultaneous pressures on each of the panels. Any calculated (quasi-static) pressure distribution must fall within the limits of these pressures.

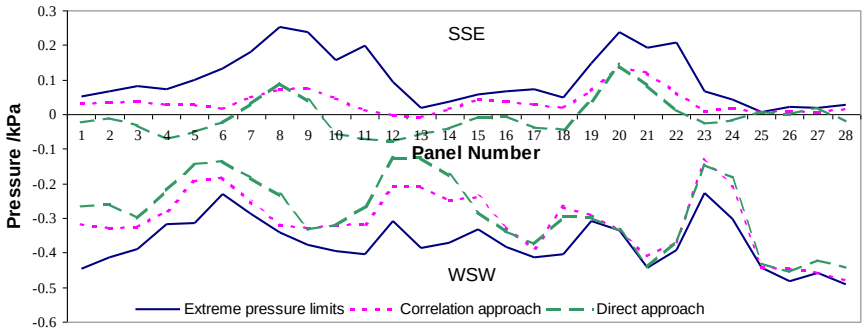

Fig. 5 Comparison of effective static pressure distributions by direct calculation and by the correlation method

6.5 Contributions from resonant dynamic response

The resonant contributions to member forces are usually small and can be approximated by adding a small percentage to the quasi-static load distributions.

For example, for the roof shown in Figure 1, a large number of resonant dynamic modes were considered to be significant contributors to the effective loads. In fact thirteen dynamic modes were included during the processing of the results. The contribution of the resonant modes varied widely between the load effects, depending on the similarity, or otherwise, of the influence lines to the mode shapes, as indicated by Equation (11). For ten load effects, the dynamic response factors varied between 1.05 and 1.69. The dynamic response factor is defined as ratio of peak load effect *including* the resonant contributions, to the peak load effect *excluding* the resonant contributions. When calculating equivalent static wind load distributions, the quasi-static distribution was simply factored by the dynamic response factor, if its value was 1.25 or less. For larger values of dynamic response factor, the more rigorous approach of Equations (17) and (18) was adopted.

7. CONCLUSIONS

Approaches developed over the last twenty years for establishing effective static wind load distributions on large roofs, typical of those on large sports facilities, have been discussed. Quasi-steady assumptions, typically used for small buildings and roofs in wind codes and standards, are not appropriate for these structures. Simple gust loading factor approaches developed for tall cantilevered structures, such as high rise buildings and towers are also not applicable.

However, wind loads on large roofs can be obtained from rigid wind-tunnel models based on pressure measurements with appropriate post-processing. The paper has discussed an analysis method based on correlation–LRC approach for the quasi-static components. Alternatively, a direct approach in which simultaneous time histories of fluctuating pressures from the whole roof are recorded and stored, can be used. These are subsequently weighted with structural influence coefficients to obtain time histories of load effects. The instantaneous pressure distributions coinciding with peak load effects are then identified and averaged.

Resonant dynamic components of wind load on large roofs are usually small. In some cases of very large roofs, however, the resonant components are significant. It is shown that the resonant contribution of a particular mode of vibration to a particular load effect depends on the similarity of the mode shape to the influence line for the load effect.

ACKNOWLEDGEMENTS

The author, and JDH Consulting, acknowledge the cooperation of many structural and wind engineering groups during the last fifteen years, including the Arup Group, Aurecon (formerly Connell-Wagner), BMT-Fluid Mechanics, MEL Consultants, MODUS, SKM, Wind Engineering Services (University of Sydney) and Windtech Consultants. This has led to greatly improved techniques for the definition of design wind loads on large roofs.

REFERENCES

Davenport, A.G. (1964), "Note on the distribution of the largest value of a random function with application to gust loading," *Proc. I.C.E.*, **19**, 449-471.

Holmes, J.D. (1990), "Analysis and synthesis of pressure fluctuations on bluff bodies using eigenvectors", *J. Wind Eng. Ind. Aerodyn.*, **33**, 219–230.

Holmes, J.D. (1992), "Optimised peak load distributions," *J. Wind Eng. Ind. Aerodyn.*, **41-44**, 267–276.

Holmes, J.D. (2002), "Effective static load distributions in wind engineering," *J. Wind Eng. Ind. Aerodyn.*, **90**, 91-109.

Holmes, J.D. (2007), *Wind loading of structures*, 2nd Edition, Taylor and Francis, London, U.K.

Holmes, J.D. and Best, R.J. (1981), "An approach to the determination of wind load effects on low-rise buildings," *J. Wind Eng. Ind. Aerodyn.*, **7**, 273-287.

Holmes, J.D. and Lewis, R.E. (1987) "Optimization of dynamic-pressure measurement systems II. – Parallel tube-manifold systems," *J. Wind Eng. Ind. Aerodyn.*, **25**(3) 275-290.

Kasperski, M. (1992), "Extreme wind load distributions for linear and nonlinear design," *Eng. Struct.*, **14,** 27-34.

Kasperski, M. and Niemann, H.-J. (1992), "The L.R.C. (Load-Response-Correlation) method: A general method of estimating unfavourable wind load distributions for linear and non-linear structural behavior", *J. Wind Eng. Ind. Aerodyn.*, **43**, 1753–1763.

Surry, D. and Stathopoulos, T. (1977), "An experimental approach to the economical measurement of spatially-averaged wind loads," *J. Ind. Aerodyn.*, **2**, 385-397.